Carbohydrate Polymers 89 (2012) 379–387

Contents lists available at SciVerse ScienceDirect

Carbohydrate Polymers

journal homepage: www.elsevier.com/locate/carbpol

RGD-conjugated UV-crosslinked chitosan scaffolds inoculated with mesenchymal stem cells for bone tissue engineering

Wei-Bor Tsai [a,*], Yi-Ru Chen [a,b], Wen-Tyng Li [c], Juin-Yih Lai [d], Hsuan-Liang Liu [b,**]

[a] Department of Chemical Engineering, National Taiwan University, No. 1, Roosevelt Rd., Sec. 4, Taipei 106, Taiwan
[b] Graduate Institute of Biotechnology and Department of Chemical Engineering and Biotechnology, National Taipei University of Technology, No. 1, Sec. 3, ZhongXiao E. Rd., Taipei 106, Taiwan
[c] Department of Biomedical Engineering, Chung Yuan Christian University, Chungli, Taoyuan, Taiwan
[d] R&D Center for Membrane Technology and Department of Chemical Engineering, Chung Yuan Christian University, Chungli, Taoyuan, Taiwan

ARTICLE INFO

Article history:
Received 3 December 2011
Received in revised form 28 February 2012
Accepted 1 March 2012
Available online 15 March 2012

Keywords:
Chitosan
Scaffold
Mesenchymal stem cells
RGD
UV-crosslinking
Bone tissue engineering

ABSTRACT

Biomimetic chitosan scaffolds were prepared using two types of chitosan derivatives, one containing photoreactive azides for UV-crosslinking and the other tethered with RGD peptides. Mesenchymal stem cells (MSCs) isolated from rat bone marrow were cultured in the RGD-conjugated, UV-crosslinked chitosan scaffolds for bone tissue engineering. RGD-incorporation to the chitosan-based scaffolds increased the cell contents from 2.4×10^4 to 3.8×10^4 cells/scaffold and 3.4×10^4 to 5.1×10^4 cells/scaffold after 1 and 10 days of culture, respectively. Furthermore, osteogenic differentiation of MSCs, indicated by ALP activity and expression of Runx2 and osteocalcin genes, was enhanced on the RGD-conjugated surface compared with the unmodified surfaces. After 14 days of osteogenic culture, calcium deposition in the RGD-conjugated scaffolds (711 nmol Ca/scaffold) was significantly higher than the control (390 nmol Ca/scaffold). The results demonstrate a potential application of RGD-immobilized, crosslinked chitosan scaffolds for bone tissue engineering applications.

1. Introduction

Chitosan, the deacetylated derivative of chitin, has been a popular material for fabricating tissue engineering scaffolds (Muzzarelli, 2009a, 2011), which allow cells to accommodate, grow, migrate and organize to form a functional tissue. Advantages of this material include its biodegradability, good biocompatibility (VandeVord et al., 2002), resemblance to glycosaminoglycans and improved mechanical properties compared to many natural polymers (Majima et al., 2005). Nevertheless, chitosan still possesses some shortcomings for such a purpose. For example, the mechanical properties of chitosan scaffolds may not be suitable to match some specific tissue engineering applications. Furthermore, chitosan lacks bioactive signals equivalent to those existing in the extracellular matrix (ECM) for cell attachment, growth and differentiation. The above problems can be improved by chemical crosslinking to improve the mechanical properties of chitosan scaffolds (Hsieh et al., 2007; Muzzarelli, 2009b), and incorporation of bioactive signals, such as ECM adhesion proteins and cell-binding peptides into chitosan substrates to enhance cell adhesion (Chung, Lu, Wang, Lin, & Chu, 2002; Ho et al., 2005; Wang, Chow, Lai, Liu, & Tsai, 2009; Wang, Chow, Tsai, & Fang, 2009).

The most commonly used cell-binding peptide sequence is arginine-glycine-aspartic acid (RGD), which is found in ECM adhesive proteins such as fibronectin and laminin (Massia & Hubbell, 1990; Pittenger et al., 1999). RGD conjugation has been shown to enhance cell attachment, growth and differentiation (Clements et al., 2011; Tsai et al., 2009; Tsai, Chen, Wei, Tan, & Lai, 2010) and is a widely used strategy in tissue engineering applications. Nevertheless, three dimensional (3D) crosslinked chitosan scaffolds with RGD conjugation are not often found in the literature regarding tissue engineering. The reason, we suspect, is that it is difficult to find a suitable protocol for the conjugation of RGD to chitosan scaffolds uniformly while crosslinking the scaffolds simultaneously.

Recently, we developed a simple and versatile method to overcome the above technical obstacles to the fabrication of RGD-conjugated, crosslinked chitosan scaffolds for bone tissue engineering (Tsai, Chen, Liu, & Lai, 2011). In this process, two chitosan derivatives were synthesized: one containing photoreactive azido groups for UV-crosslinking (Chien, Chang, & Tsai, 2009) and the other tethered with RGD peptides. The solution of two chitosan derivatives was fabricated into scaffolds by freeze-drying and subsequent UV crosslinking. We showed that the mechanical

* Corresponding author. Tel.: +886 2 3366 3996; fax: +886 2 2362 3040.
** Corresponding author.
E-mail addresses: weibortsai@ntu.edu.tw (W.-B. Tsai), med403@gmail.com (Y.-R. Chen), wtli@cycu.ntu.edu (W.-T. Li), jylai@cycu.edu.tw (J.-Y. Lai), f10894@ntut.edu.tw (H.-L. Liu).

0144-8617/$ – see front matter © 2012 Elsevier Ltd. All rights reserved.
doi:10.1016/j.carbpol.2012.03.017

properties and pore structures of chitosan scaffolds can be tuned by controlling the content of crosslinkers. Attachment, proliferation and differentiation of osteoblasts were all significantly enhanced in the RGD-conjugated chitosan scaffolds compared to unmodified scaffolds, demonstrating the potential of our technique in regard to the preparation of chitosan-based scaffolds for tissue engineering.

This study was aimed at applying RGD-conjugated chitosan scaffolds combined with bone marrow stromal cells, also referred to as mesenchymal stem cells (MSCs), to bone tissue engineering. The cells possess the ability of extensive self-renewal and differentiation along the osteogenic and various other cell lineages (Caplan, 1991; Pittenger et al., 1999), and play a pivotal role in bone regeneration and repair *in vivo* (Phillips, 2005). Chitosan has been reported to be a suitable substrate for the culture and differentiation of MSCs (Mathews, Gupta, Bhonde, & Totey, 2011; Venkatesan & Kim, 2010; Yang, Chen, & Wang, 2009). On the other hand, RGD-containing peptides are known to be capable of promoting osteogenesis of MSCs in poly(ethylene glycol)-based hydrogels (Shin et al., 2005; Yang et al., 2005), and chitosan films (Lee et al., 2009). Nevertheless, culture and osteogenic differentiation of MSCs in 3D RGD-containing chitosan scaffolds has not been reported. In this study, mouse MSCs were isolated and cultured in RGD-modified UV-crosslinked chitosan substrates. The effect of RGD-incorporation on the attachment, growth and osteogenesis of MSCs was then evaluated with regard to the suitability of this material for bone tissue engineering applications.

2. Materials and methods

2.1. Materials

Reagents were purchased from Sigma–Aldrich (USA) unless specified otherwise. *N*-(3-dimethylaminopropyl)-*N*'-ethylcarbodiimide hydrochloride was purchased from Fluka (USA). RGD-peptide (*N*-acetyl-G**RGD**SPGYG-amide) was obtained from Kelowna International Scientific Inc. (Taipei, Taiwan). The peptide concentration was calculated from the absorbance at 275 nm which is characteristic for the tyrosine residue (Y, molar adsorption coefficient 1420 M^{-1} cm^{-1}).

MSC culture medium consisted of 90% (v/v) low glucose DMEM, 2 mM L-glutamine, 100 U/mL penicillin, 100 μg/mL streptomycin, 250 ng/mL amphotericin B, 0.1 mM MEM nonessential amino acid, 3.7 g/mL sodium bicarbonate, and 10% FBS, pH 7.4. The MSC culture medium supplemented with 0.1 μM dexamethasone, 1 mM β-glycerophosphate and 50 μg/mL ascorbic acid comprised osteogenic medium. Red blood cell lysis buffer consisted of 150 mM ammonium chloride, 10 mM potassium bicarbonate, 0.1 mM EDTA disodium salt.

2.2. Conjugation of phenylazide groups and peptides to chitosan

Photoreactive azido groups were conjugated to chitosan (molecular weight 50–190 kDa, 75–85% deacetylation) via a reaction forming covalent amide bonds between the amino groups of chitosan and the carboxyl groups of an azidobenzoic acid ester. Briefly, 5-azido-2-nitrobenzoic acid N-hydroxysuccinimide ester (47 mg; cat. No. A3282, Sigma) was dissolved in 0.2 mL of dimethylsulfoxide and then mixed with the chitosan solution (0.1 g chitosan in 4.8 mL of 1% acetic acid). *N*-(3-dimethylaminopropyl)-*N*'-ethylcarbodiimide hydrochloride (61 mg) and N-hydroxysuccinimide (33.5 mg) were then added and incubated at room temperature for 3 h. Unreacted chemicals were removed by dialysis against deionized water through a cellulose tube (MWCO 12,400 Da) in the dark for two days with changes of fresh deionized water every 12 h. After freeze-drying, the azide-conjugated chitosan (CHI-g-AZ) was kept at 4 °C until further use.

The content of azido groups in CHI-g-AZ was determined by ^{1}H nuclear magnetic resonance (^{1}H NMR, Avance-500MHz, Bruker), as shown in Fig. A1 of the Appendix. The molar percentage of the azido groups in CHI-g-AZ was estimated to be 3.8 mol% of the amino groups of chitosan, calculated from the ratio of the peak areas of the aromatic protons at 6.84–8 ppm to the –C<u>H</u>–NH_2 proton at 2.86 ppm, according to a previous study (Tsai et al., 2011).

RGD peptides were conjugated onto chitosan molecules via a carbodiimide reaction according to a previously developed procedure (Tsai et al., 2011). The graft ratio of RGD to chitosan (CHI-g-RGD) was estimated as 2.75 mol% with respect to the total moles of the amino groups of chitosan molecules, as described in a previous study (Tsai et al., 2011).

2.3. Preparation of chitosan films and scaffolds

Mixtures of unmodified chitosan, CHI-g-AZ and CHI-g-RGD with a total concentration of 10 mg/mL in 1% acetic acid, were prepared at weight percentages (%) as listed below:

Types of films or scaffolds	Chitosan	CHI-g-AZ	CHI-g-RGD
Chitosan	100	0	0
c-Chitosan	50	50	0
c-Chitosan-RGD	46	50	4

The preparation of chitosan films started with adding 70 μL/well of the chitosan mixture in 96-well TCPS plates, which were then allowed to dry in air at room temperature. Chitosan scaffolds were prepared by freeze-drying. Briefly, the chitosan mixture was poured into 96-well TCPS plates (70 μL/well for cell culture experiments and 336 μL/well for mechanical testing), followed by freeze drying in the dark to form scaffolds. Subsequently, chitosan substrates were crosslinked by UV irradiation for 30 min (12 cm below a halogen UV lamp, wavelength range 280–380 nm). A light intensity of 65 mW/cm^2 was determined at this distance using a UV radiometer.

2.4. Characterization of chitosan scaffolds

The porous structure of chitosan scaffolds was investigated by scanning electron microscopy (SEM) images (JSM-5310, JEOL, Japan) according to a previous procedure (Wang, Chow, Tsai, et al., 2009). Average pore sizes of each type of scaffold were determined from more than 100 pores.

The compressive stress–strain properties of chitosan scaffolds was determined using a compressive testing machine (FGS-50V-H, NIDECSIMPO Corporation, Japan) and a digital force gauge (FGP-0.5, NIDECSIMPO Corporation, Japan), according to a previous procedure (Tsai et al., 2011).

2.5. Culture of MSCs

Standard sterile cell culture techniques were used for all cell experiments. The animal procedure followed the ethical guidelines of Care and Use of Laboratory Animals (National Taiwan University, National Institutes of Health Publication No. 85-23, revised 1985) and was approved by the Animal Center Committee of National Taiwan University. Mesenchymal stem cells (MSCs) were isolated from femurs and tibias of female Wistar rats (~100 g) according to a previously published procedure (Wang, Tsai, & Voelcker, 2012). Cells at passage 3 were used in this study. The cells tested positive for their ability to differentiate to bone-like (Alizarin Red-positive) and lipid containing (Oil Red-positive) cells and therefore were considered as MSCs (Javazon, Colter, Schwarz, & Prockop, 2001).

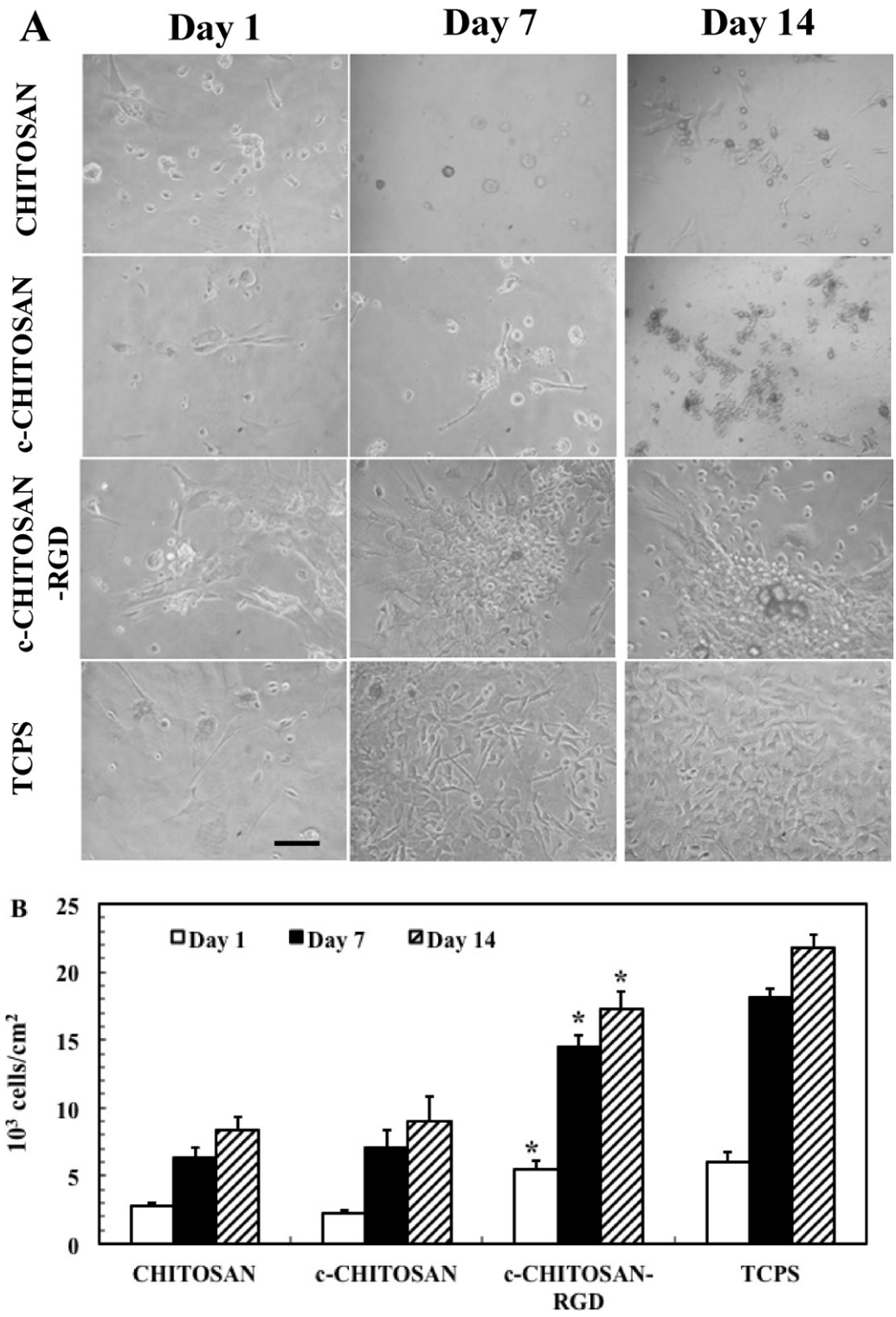

Fig. 1. MSCs cells were cultured on CHITOSAN, c-CHITOSAN and c-CHITOSAN-RGD films for 1, 7 and 14 days of incubation in the MSC culture medium. (A) Phase contrast microscopic images of MSCs (magnification 200×). The scale bar in the images represents 100 μm. (B) The number of MSCs. The values represent mean ± standard deviation, $n = 4$. * indicates $p < 0.001$ vs. CHITOSAN and c-CHITOSAN at the same culture period. Tissue culture polystyrene (TCPS) was used as a control.

Prior to cell seeding, the chitosan samples were soaked in 70% ethanol for 30 min, followed by three rinses with sterilized PBS. For cell culture on chitosan films, the cells suspended in the MSC culture medium (8×10^4 cells/mL) were added onto the chitosan films (50 μL/well), making the seeding density 1.25×10^4 cells per cm^2. The cell morphology was observed under a phase contrast microscope. For cell culture in chitosan scaffolds, 50 μL of a MSC suspension (6×10^6 cells/mL) was inoculated into the chitosan scaffolds, making the seeding density 3×10^5 cells per scaffold.

The cell numbers in chitosan films or scaffolds were determined by a lactate dehydrogenase (LDH) assay, which was modified from a previous procedure (Grunkemeier, Tsai, Alexander, Castner, & Horbett, 2000) and reported previously (Tsai et al., 2010). Intracellular ALP activities were assayed by determining the release of

p-nitrophenol from 4-nitrophenyl phosphate disodium salt at pH 10.2, as reported previously (Tsai et al., 2009).

2.6. Reverse-transcription polymerase chain reaction (RT-PCR) for analysis of the expression of osteogenic genes

After MSCs were cultured on chitosan films in the osteogenic medium for 2 or 3 weeks, the expression of Runx2 and osteocalcin (OCN) genes was analyzed by RT-PCR. The extraction of mRNA and the preparation of complementary DNA (cDNA) were performed according to a previous procedure (Tsai, Chen, Chen, & Chang, 2006). PCR was performed in a thermocycler (PS320, ASTEC, Japan) by using Taq polymerase (M1865, PROMEGA, Taiwan).

The sequences of PCR primers (forward and backward, 5′ to 3′) were (the numbers in parenthesis indicating the length of PCR products/annealing temperature/cycle number): glyceraldehyde-3-phosphate dehydrogenase (GAPDH), 5′-ACCACAGTCCATGCCATCAC-3′ and 5′-TCCACCACCCTGTTGCTGTA-3′ (452 bp/60 °C/35); Runx2, 5′-GCTTCATTCGCCTCACAAACA-3′ and 5′-TGCTGTCCTCCTGGAGAAAGTT-3′ (387 bp/52 °C/40); OCN, 5′-GTCCCACACAGCAACTCG-3′ and 5′-CCAAAGCTGAAGCTGCCG-3′ (611 bp/61 °C/24).

The PCR operation profile included initial denaturation at 94 °C for 10 min, the desired cycle numbers of denaturation at 94 °C for 30 s, annealing for 30 s, and extension at 72 °C for 30 s, and final extension at 72 °C for 5 min. PCR products were analyzed by separating in a 2% agarose gel, followed by staining with ethidium bromide solution for 30 min. The images of electrophoresis gels were taken under UV light and the band intensity of every PCR product was quantified by NIH Image J. The intensities of the bands for Runx2 and OCN were first normalized to that of GAPDH from the same sample, and then divided by the value on TCPS on the same day.

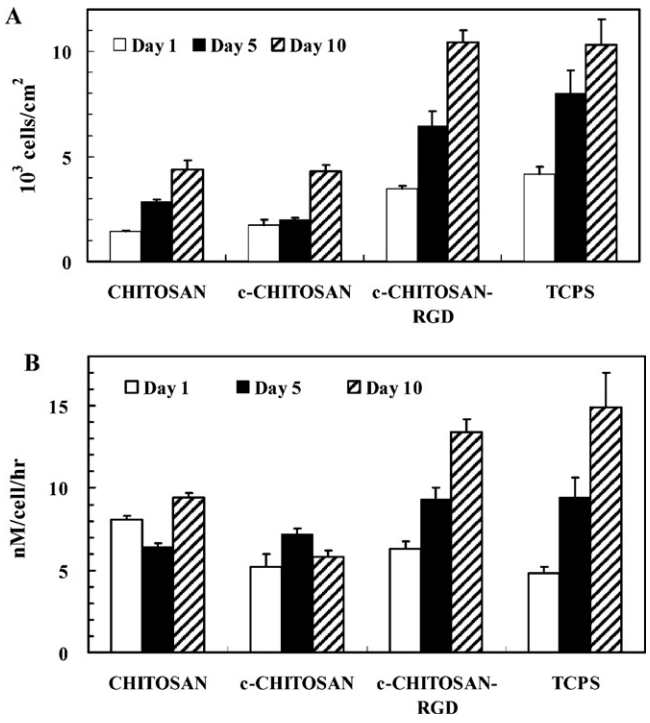

Fig. 2. MSCs were seeded on CHITOSAN, c-CHITOSAN and c-CHITOSAN-RGD films for 1 day, followed by 1, 5 and 10 days of osteogenic culture: (A) the number and (B) the alkaline phosphatase activity of MSCs. The values represent mean ± standard deviation, $n = 4$. * indicates $p < 0.001$ vs. CHITOSAN and c-CHITOSAN at the same culture period. # indicates $p < 0.01$ vs. CHITOSAN on Day 1. Tissue culture polystyrene (TCPS) was used as a control.

2.7. Mineralization culture of the MSC/scaffold constructs

The MSC/scaffold constructs were seeded in the MSC culture medium for 1 day, followed by culture in the osteogenic medium for 1, 5 or 10 days with daily replenishment of freshly L-ascorbate (50 μg/mL). Calcium deposition was analyzed by determination of the calcium content and histological analysis. The total amount of calcium deposition was determined using a calcium assay kit (Diagnostic Chemicals Limited, USA) according to a previous protocol (Tsai et al., 2010). The preparation of histological samples of MSC/scaffold constructs and the staining of histological samples of Alizarin red S followed a previous procedure (Tsai et al., 2011).

2.8. Statistical analysis

Each experiment has been repeated at least three times. Statistical assessment of significant variations was performed by GraphPad Instat® 3.00 (GraphPad Software Inc.). Significance was assessed by one way analysis of variance (ANOVA) and two-tailed Student–Newman–Keuls multiple comparison. A probability of $p \leq 0.05$ was considered a significant difference.

3. Results and discussion

3.1. The attachment, growth and osteogenic differentiation of MSCs on RGD-conjugated chitosan films

First of all, we evaluated whether RGD conjugation via our method possessed the capability of enhancing the attachment, proliferation and osteogenic differentiation of MSCs. The cells were first cultured on 2D chitosan films without osteogenic induction to evaluate their adhesion and proliferation. After incubation in the MSC culture medium for 1 or 7 days, few cells were found to attach and spread on Chitosan and c-Chitosan, while most of those on c-Chitosan-RGD displayed elongated and spread morphology (Fig. 1A). Furthermore, MSCs tended to form aggregates on c-Chitosan-RGD after 7 or 14 days of incubation, in contrast to those on TCPS remaining their spread morphology without formation of aggregates.

Quantification of cell numbers indicated that RGD incorporation in the chitosan films increased one-day cell attachment to 5.4×10^3 cells/cm^2, significantly higher than the cell numbers observed on Chitosan and c-Chitosan (2.7 and 2.2×10^3 cells/cm^2, respectively) (Fig. 1B, $p < 0.001$). After 7 days of culture, the cell numbers on c-Chitosan-RGD was increased to 14.4×10^3 cells/cm^2, roughly twice the number observed on Chitosan (6.3×10^3 cells/cm^2) or c-Chitosan (7.1×10^3 cells/cm^2) (Fig. 1B, $p < 0.001$). This trend remained after 14 days of culture. The results indicated that RGD conjugation by our method maintained the ability to enhance the attachment and proliferation of MSCs on chitosan films over this time frame.

Next, the efficacy of RGD-conjugated chitosan on proliferation and osteogenic differentiation of MSCs was investigated under osteogenic culture. MSCs were seeded and cultured in the MSC culture medium for 1 day, followed by culture in the osteogenic medium for 1, 5 and 10 days. Cellular morphology after the osteogenic culture was very similar to that in the MSC culture medium, except that no cell aggregate was found on c-Chitosan-RGD (microscopic images shown in Fig. A2 of Appendix). Incorporation of RGD increased not only 1-day cell attachment but also cell proliferation in the osteogenic medium (Fig. 2A). After 5 days of culture, the cell number on c-Chitosan-RGD was 6.4×10^3/cm^2, representing an almost three fold increase compared to the values observed on Chitosan or c-Chitosan (2.8 and 2.0×10^3 cells/cm^2, respectively; $p < 0.001$). After 10 days of culture, the cell numbers between Chitosan and c-Chitosan were still

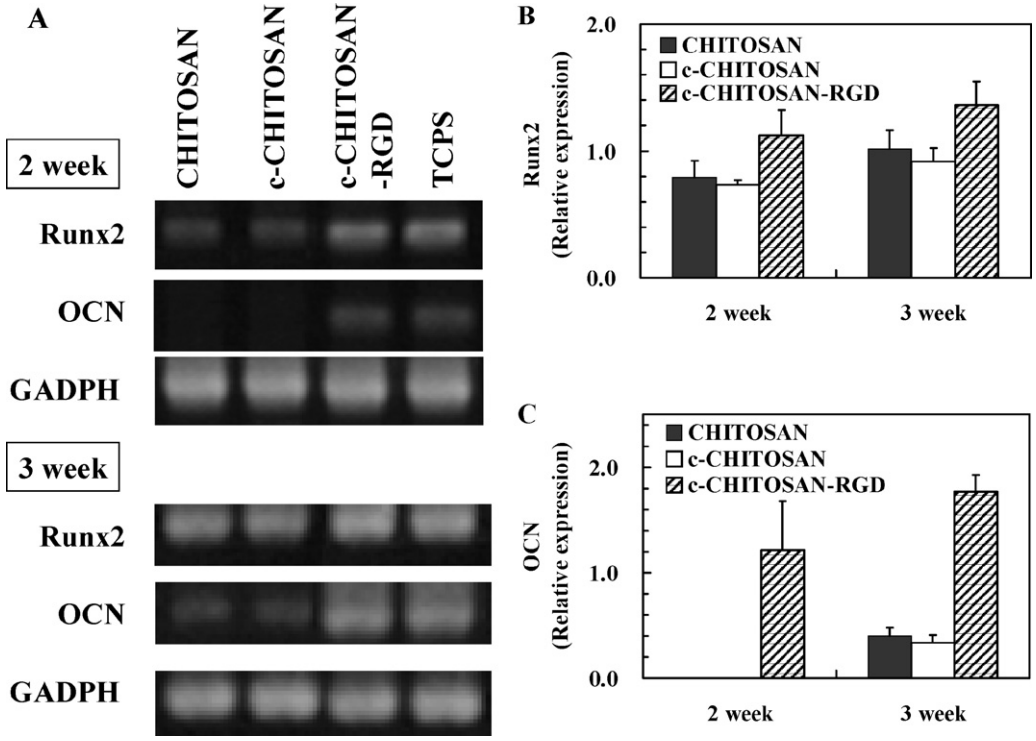

Fig. 3. After cultured in the osteogenic medium for 2 or 3 weeks on CHITOSAN, c-CHITOSAN and c-CHITOSAN-RGD, the expression of Runx2. osteocalcin (OCN) and GADPH of MSCs was determined by RT-PCR. (A) Electrophoresis images for the RT-PCR products of Runx2, OCN and GADPH. Tissue culture polystyrene (TCPS) was used as a control. The intensities of the bands for Runx2 and OCN were first normalized to that of GAPDH from the same sample, and then divided by the value on TCPS on the same day: the normalized band intensity for (B) Runx2 and (C) OCN.

comparable (4.3 and 4.2×10^3 cells/cm^2, respectively), and much smaller than that those on c-Chitosan-RGD (10.4×10^3 cells/cm^2, $p < 0.001$).

The osteogenic differentiation of MSCs on the chitosan films was analyzed by several early and late osteogenic markers. Alkaline phosphatase (ALP), an essential enzyme for ossification, is an early bone marker protein and one of the most frequently used markers to demonstrate osteoblast differentiation (Grunkemeier et al., 2000). Runx2 (also known as Cbfa1), a transcription factor, has been suggested to be the 'master switch' responsible for initiation of osteoblast differentiation from MSCs (Otto et al., 1997). Runx2 plays a pivotal role in bone formation through the transcriptional regulation of its target genes at developmental transitions. Osteocalcin (OCN), a 10-kDa non-collagenous bone-specific protein, is exclusively secreted by mature osteoblasts towards the end of mineralization and is thought to be a late-stage differentiation marker (Makita et al., 2008; Yang et al., 2005). Together, Runx2 and OCN are the early and late regulators of osteoblast differentiation and functions (Ducy, 2000; Schroeder, Jensen, & Westendorf, 2005). The final stage of osteoblast differentiation is mineralization, at which mineral matrix containing mainly calcium phosphate is secreted and deposited by mature osteoblasts.

After osteogenic culture for 5 days, the cellular ALP activity on c-Chitosan-RGD (9.3 nM/cell/h) was significantly higher than those on Chitosan (6.5 nM/cell/h) and c-Chitosan (7.2 nM/cell/h) (Fig. 2B, $p < 0.001$). After 10 days of osteogenic culture, the enhancement was further enlarged by c-Chitosan-RGD (14.9 nM/cell/h) compared with Chitosan (9.43 nM/cell/h) or c-Chitosan (5.8 nM/cell/h) (Fig. 2B, $p < 0.001$).

The expression of Runx2 and OCN genes was analyzed by RT-PCR. The expression of both genes was not detected on all three types of chitosan films until 2 weeks of osteogenic culture. Runx2 was expressed on all three types of samples, but to a higher extent on c-Chitosan-RGD (Fig. 3A). On the other hand, the expression of OCN was not obvious on Chitosan and c-Chitosan, but detectable on c-Chitosan-RGD. After 3 weeks of osteogenic culture, the level of Runx2 expression on Chitosan and c-Chitosan was increased to a level comparable to that on c-Chitosan-RGD. The expression of OCN was detectable on Chitosan and c-Chitosan at this time, but the level was still much lower when compared with c-Chitosan-RGD. The quantitative analysis of gene expression indicated that the expression of Runx2 on c-Chitosan-RGD was significantly higher than those on Chitosan and c-Chitosan after two weeks of osteogenic culture (Fig. 3B). The expression of Runx2 was increased on all substrates during the third week of osteogenic culture, but was still higher on c-Chitosan-RGD. The expression of OCN was much higher on c-Chitosan-RGD compared to Chitosan and c-Chitosan after 2 and 3 weeks of osteogenic culture (Fig. 3C). The expression of Runx2 and OCN was only better on c-Chitosan-RGD when compared to TCPS. These results demonstrate that RGD increases the transcript levels of the early osteogenesis marker, Runx2, which in turn up-regulates the OCN promoter activity (Makita et al., 2008).

After the MSCs were cultured in the osteogenic medium for 2 weeks, more red Alizarin red S-stained spots were found on c-Chitosan-RGD compared to the other two types of chitosan samples (Fig. 4A). The total amounts of calcium on Chitosan and c-Chitosan were quantified as 81 and 74 nmol/well, much less than the amount observed on c-Chitosan-RGD (155.17 nmol/well, Fig. 4B; $p < 0.001$). Our results therefore indicate that calcium deposition was better on c-Chitosan-RGD.

The results on 2D chitosan films demonstrate that azido crosslinking does not adversely affect the adhesion, proliferation and osteogenic differentiation of MSCs on chitosan films. Furthermore, RGD conjugation significantly enhances the performance of MSCs on chitosan films. Therefore, the applicability of crosslinked

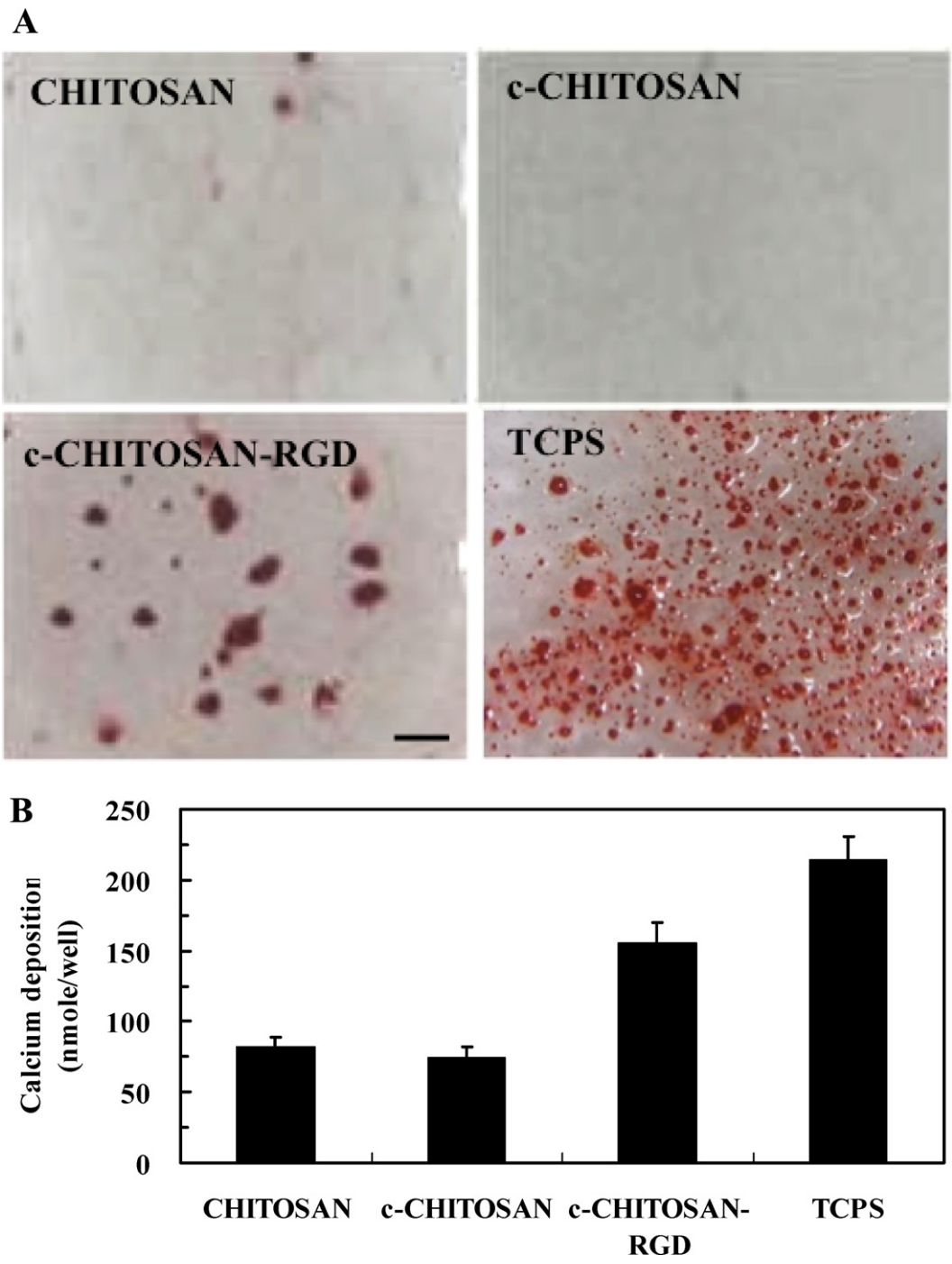

Fig. 4. (A) The images of MSC culture on CHITOSAN, c-CHITOSAN and c-CHITOSAN-RGD for 14 days of osteogenic culture, followed by Alizarin red staining. The images were taken from a digital camera. The scale bar represents 0.5 mm. (B) Quantitative calcium deposition by MSCs on CHITOSAN, c-CHITOSAN and c-CHITOSAN-RGD after 14 days of osteogenic culture. The values represent mean ± standard deviation, $n = 4$. * indicates $p < 0.001$ vs. CHITOSAN and c-CHITOSAN. Tissue culture polystyrene (TCPS) was used as a control.

RGD-containing 3D chitosan scaffolds in bone tissue engineering applications was next evaluated.

3.2. Fabrication and characterization of UV-crosslinked RGD-containing chitosan scaffolds

The porous structure of the chitosan-based scaffolds, examined by SEM, was similar with an open inter-connective pore microstructure (Fig. 5A). No obvious difference was found among different scaffolds. The average pore size in Chitosan was approximately 104 μm, which was significantly smaller than the pore size observed in c-Chitosan and c-Chitosan-RGD scaffolds (approximately 124 μm) (Fig. 5B, $p < 0.05$).

The compressive stress–strain plots of these chitosan scaffolds are shown in Fig. A3 of the Appendix. UV-crosslinking increased the compressive stress at 95% strain from 3.39 MPa for Chitosan to 9.08 MPa for c-Chitosan (Fig. 5C, $p < 0.001$), while RGD incorporation did not influence the compressive properties of c-Chitosan. The equilibrium stress of these three types of chitosan scaffolds displayed a similar trend. The results show that UV-crosslinking via azido groups enhances the mechanical properties of chitosan scaffolds.

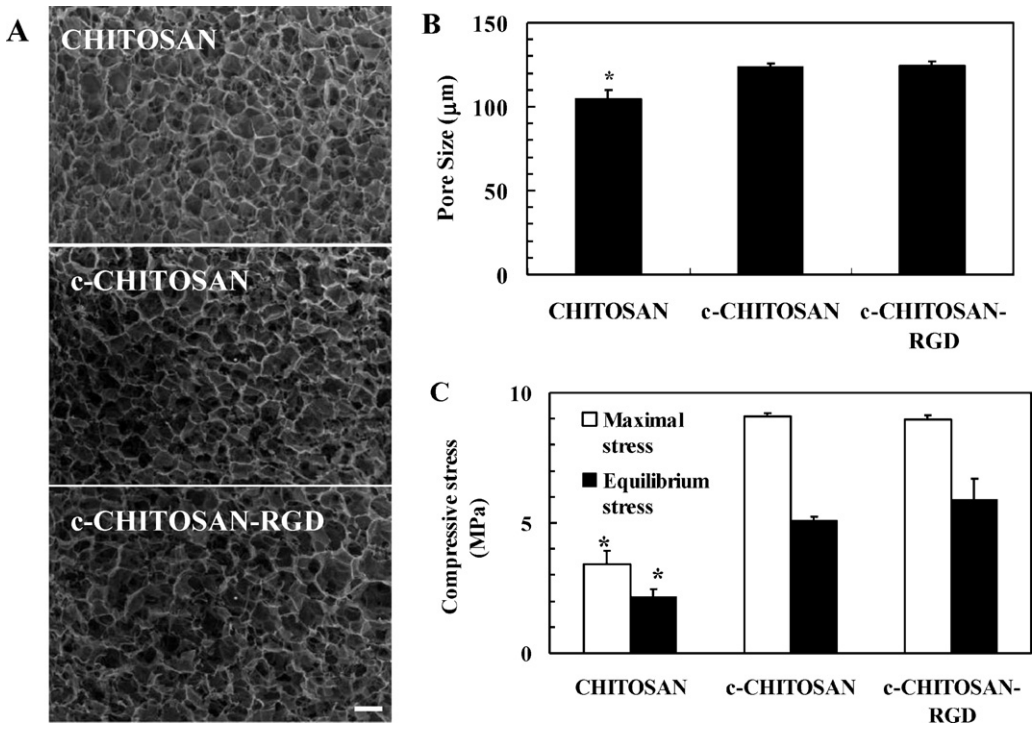

Fig. 5. (A) The SEM images of CHITOSAN, c-CHITOSAN and c-CHITOSAN-RGD scaffolds. The scale bar represents 100 μm. (B) The average pore diameters of the chitosan-based scaffolds. The data represent mean ± standard error of the mean, $n > 100$. $p < 0.05$ vs. c-CHITOSAN and c-CHITOSAN-RGD. (C) The maximal compressive stresses of the chitosan-based scaffolds at 95% strain and the equilibrium stresses after relaxation. The values represent mean ± standard deviation, $n = 4$. $p < 0.001$ vs. c-CHITOSAN and c-CHITOSAN-RGD.

3.3. Culture of MSCs in RGD-incorporated chitosan scaffolds for bone tissue engineering

MSCs were seeded and cultured in the chitosan-based scaffolds for 1 day in the MSC culture medium, followed by osteogenic culture for 1, 5 or 10 days. After one-day culture, cell attachment to c-Chitosan-RGD (3.8×10^4 cells/scaffold) was significantly higher compared to Chitosan and c-Chitosan (2.38 and 2.35×10^4 cells/scaffolds, respectively) (Fig. 6A, $p < 0.001$). After 5 days of osteogenic culture, the cell numbers in Chitosan and c-Chitosan were still comparable (2.7 and 2.4×10^4 cells/scaffold, respectively), while the cell number in c-Chitosan-RGD was increased to 4.15×10^4 cells/scaffold ($p < 0.05$). After 10 days of osteogenic culture, the cell numbers in Chitosan and c-Chitosan scaffolds were still similar (3.4 and 3.3×10^4 cells/scaffold, respectively), and smaller than the cell number in c-Chitosan-RGD (5.14×10^4 cells/scaffold, $p < 0.001$).

After 1 day of osteogenic incubation, the ALP activity in the c-Chitosan-RGD scaffolds (10.50 nM/cell/h) was slightly higher than Chitosan and c-Chitosan (8.33 and 8.62 nM/cell/h, respectively) (Fig. 6B). After 5 days of osteogenic culture, the ALP activity was increased in all scaffolds, while that in c-Chitosan-RGD (16.03 nM/cell/h) was still higher than the other two types (~10.50 nM/cell/h). The ALP activity continued to increase on all substrates for 10 days of culture. The ALP activity on c-Chitosan-RGD (19.54 nM/cell/h) remained the highest among all types of chitosan scaffolds ($p < 0.05$).

After 14 days of osteogenic culture, more red Alizarin red S-stained regions were found on c-Chitosan-RGD compared to the other two types of chitosan samples (Fig. 7A), suggesting that more calcium was deposited by the MSCs cultured in c-Chitosan-RGD. No obvious difference in the red-staining areas in the central and peripheral portion of c-Chitosan-RGD scaffolds was found, while the red-staining area was more profound in the peripheral

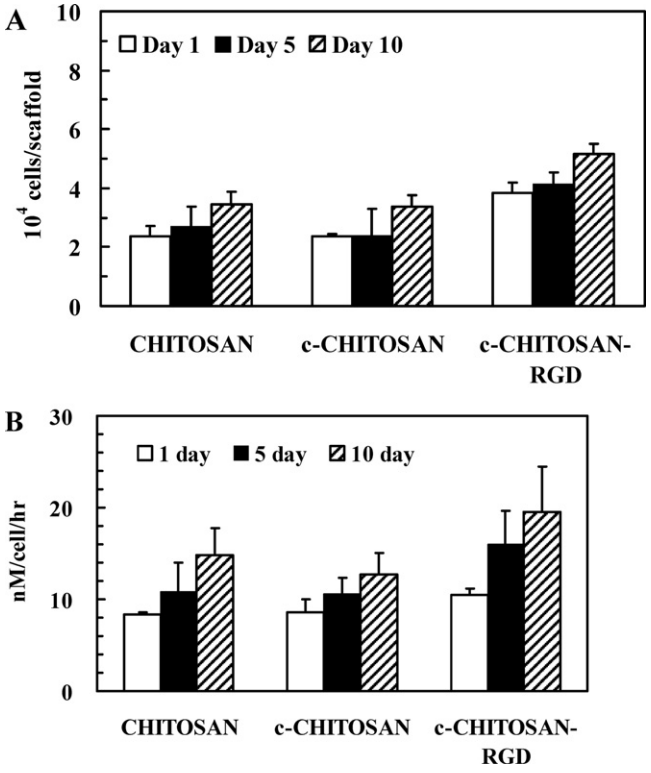

Fig. 6. (A) The number and (B) the alkaline phosphatase activity of MSCs in CHITOSAN, c-CHITOSAN and c-CHITOSAN-RGD scaffolds after at 1, 5 and 10 days of osteogenic culture. The values represent mean ± standard deviation, $n = 4$. * and ** indicates $p < 0.05$ and 0.001, respectively, vs. CHITOSAN and c-CHITOSAN at the same culture period.

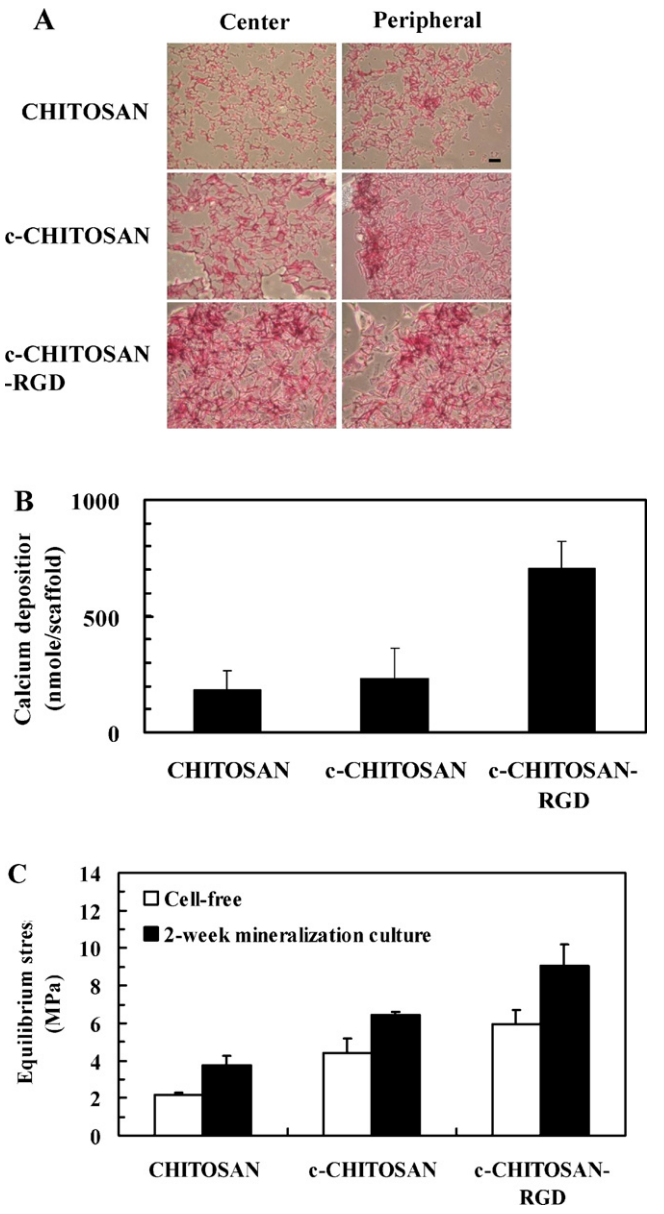

Fig. 7. MSCs were cultured in CHITOSAN, c-CHITOSAN and c-CHITOSAN-RGD scaffolds for 14 days in the osteogenic medium. (A) The images of the dissection of MSC/scaffold constructs, stained by Alizarin red staining. The scale bar represents 100 μm. (B) Quantitative calcium deposition by MSCs in CHITOSAN, c-CHITOSAN and c-CHITOSAN-RGD scaffolds. The values represent mean ± standard deviation, $n = 4$. * indicates $p < 0.001$ vs. CHITOSAN and c-CHITOSAN. (C) The maximal compressive stresses of the chitosan-based scaffolds at 95% strain before or after cell culture. The values represent mean ± standard deviation, $n = 4$. * indicates $p < 0.001$ vs. c-CHITOSAN-RGD.

region compared to the center of Chitosan and c-Chitosan. This observation suggests that RGD conjugation facilitates the penetration of MSCs into chitosan scaffolds as well as osteoblast activity. The quantified data of calcium deposition also indicated that the calcium content in c-CHITOSAN-RGD (711 nmol/scaffold) was significantly higher than the calcium content in Chitosan and c-Chitosan (387 and 297 nmol/scaffold, respectively) (Fig. 7B, $p < 0.001$).

The compressive properties of the bone tissue engineered constructs were also analyzed. The inoculation of MSCs and 14-day osteogenic culture increased the maximum compressive stress of Chitosan scaffolds from 3.13 MPa to 5.87 MPa (Fig. 7C). Similarly, the maximum compressive stress of c-Chitosan scaffolds was increased from 9.68 MPa to 11.42 MPa after cell culture. Nevertheless, c-Chitosan-RGD scaffolds possessed the highest compressive stress after mineralization culture (13.6 MPa, $p < 0.001$ vs. Chitosan and c-Chitosan).

The above results clearly demonstrate that RGD conjugation benefits bone tissue engineering in 3D chitosan scaffolds. The behavior of MSCs in regard to attachment, proliferation, osteogenic differentiation and mineralization was enhanced in RGD-conjugated incorporation chitosan scaffolds. The mechanical properties of chitosan scaffolds after cell culture were enhanced by UV-crosslinking and RGD conjugation. Therefore, crosslinked RGD-containing chitosan scaffolds combined with MSCs are expected to be advantageous in bone tissue engineering applications.

3.4. Application of RGD-conjugated chitosan scaffolds in bone tissue engineering

The development of scaffolds to support and regulate bone regeneration by functioning as the structural part of the ECM and maintaining the space and shape of the defect is still a major concern in tissue engineering research. In this field, Chitosan, which is structurally similar to hyaluronic acid of the ECM (Peniche et al., 2007), is thought to be suited for the application as a base material in tissue engineering. Chitosan is suggested to possess osteogenic properties and suitable for the tissue engineering of bone (Mathews et al., 2011; Yang et al., 2009). Immobilization of RGD on chitosan molecules to enhance chitosan's cellular affinity has been demonstrated on two-dimensional film structures (Chung et al., 2002; Hacker et al., 2003), but rarely in three-dimensional scaffolds. In this study, we demonstrated that the proliferation and differentiation of MSCs were enhanced on RGD-conjugated crosslinked chitosan scaffolds, which thus possess a high potential for bone tissue engineering.

A new method for the preparation of RGD-conjugated, crosslinked chitosan scaffolds was applied in this study. This method possesses several advantages over the commonly used strategy, post-conjugation, by which RGD peptides are conjugated to pre-formed chitosan scaffolds via suitable chemical reactions (e.g. amide bond-forming reactions) to the amino or hydroxyl groups of chitosan (Ho et al., 2005). Several drawbacks of the post-conjugation strategy, such as difficulty in precise control of the density of conjugated RGD and uniform distribution of RGD peptides throughout chitosan scaffolds, could be overcome by our method. RGD peptides are first conjugated onto chitosan molecules prior to scaffold fabrication. As we expected, MSCs grew into the center of the c-Chitosan-RGD scaffolds and deposited calcium minerals (Fig. 7), indicating that our RGD-conjugated chitosan scaffolds enhance cellular penetration and function inside the chitosan scaffolds. Furthermore, our method provides simultaneous crosslinking and peptide-conjugation in chitosan scaffolds. Therefore, chitosan scaffolds are strengthened and bio-functionalized at the same time, which benefits their application to regeneration medicine.

4. Conclusion

The suitability of RGD-conjugated UV-crosslinked chitosan scaffolds for bone tissue engineering applications has been demonstrated in this study. Rat MSCs showed improved attachment and proliferation on RGD-conjugated chitosan substrates compared to unmodified substrates. Furthermore, MSCs showed progressive osteogenesis in RGD-conjugated chitosan scaffolds. Taken together, these results indicate that the conjugation of RGD peptides to chitosan scaffolds leads to a favorable microenvironment

for MSCs, which promotes the proliferation and/or differentiation into osteoblasts and the production of mineralized matrix.

Acknowledgments

The authors gratefully acknowledge financial support from the National Science Council, Taiwan (Grant No.: 99-2221-E-002-131). The authors wish to thank Dr. Helmut Thissen (CSIRO, Clayton, Australia) for critical discussion and English editing of the manuscript.

Appendix A. Supplementary data

Supplementary data associated with this article can be found, in the online version, at doi:10.1016/j.carbpol.2012.03.017.

References

Caplan, A. I. (1991). Mesenchymal stem cells. *Journal of Orthopaedic Research*, *9*(5), 641–650.

Chien, H. W., Chang, T. Y., & Tsai, W. B. (2009). Spatial control of cellular adhesion using photo-crosslinked micropatterned polyelectrolyte multilayer films. *Biomaterials*, *30*(12), 2209–2218.

Chung, T. W., Lu, Y. F., Wang, S. S., Lin, Y. S., & Chu, S. H. (2002). Growth of human endothelial cells on photochemically grafted Gly-Arg-Gly-Asp (GRGD) chitosans. *Biomaterials*, *23*(24), 4803–4809.

Clements, L. R., Wang, P. Y., Harding, F., Tsai, W. B., Thissen, H., & Voelcker, N. H. (2011). Mesenchymal stem cell attachment to peptide density gradients on porous silicon generated by electrografting. *Physica Status Solidi A – Applications and Materials Science*, *208*(6), 1440–1445.

Ducy, P. (2000). Cbfa1: A molecular switch in osteoblast biology. *Developmental Dynamics*, *219*(4), 461–471.

Grunkemeier, J. M., Tsai, W. B., Alexander, M. R., Castner, D. G., & Horbett, T. A. (2000). Platelet adhesion and procoagulant activity induced by contact with radiofrequency glow discharge polymers: Roles of adsorbed fibrinogen and vWF. *Journal of Biomedical Materials Research*, *51*(4), 669–679.

Hacker, M., Tessmar, J., Neubauer, M., Blaimer, A., Blunk, T., Gopferich, A., et al. (2003). Towards biomimetic scaffolds: anhydrous scaffold fabrication from biodegradable amine-reactive diblock copolymers. *Biomaterials*, *24*(24), 4459–4473.

Ho, M. H., Wang, D. M., Hsieh, H. J., Liu, H. C., Hsien, T. Y., Lai, J. Y., et al. (2005). Preparation and characterization of RGD-immobilized chitosan scaffolds. *Biomaterials*, *26*(16), 3197–3206.

Hsieh, C. Y., Tsai, S. P., Ho, M. H., Wang, D. M., Liu, C. E., Hsieh, C. H., et al. (2007). Analysis of freeze-gelation and cross-linking processes for preparing porous chitosan scaffolds. *Carbohydrate Polymers*, *67*(1), 124–132.

Javazon, E. H., Colter, D. C., Schwarz, E. J., & Prockop, D. J. (2001). Rat marrow stromal cells are more sensitive to plating density and expand more rapidly from single-cell-derived colonies than human marrow stromal cells. *Stem Cells*, *19*(3), 219–225.

Lee, J. Y., Choo, J. E., Choi, Y. S., Shim, I. K., Lee, S. J., Seol, Y. J., et al. (2009). Effect of immobilized cell-binding peptides on chitosan membranes for osteoblastic differentiation of mesenchymal stem cells. *Biotechnology and Applied Biochemistry*, *52*, 69–77.

Majima, T., Funakosi, T., Iwasaki, N., Yamane, S. T., Harada, K., Nonaka, S., et al. (2005). Alginate and chitosan polyion complex hybrid fibers for scaffolds in ligament and tendon tissue engineering. *Journal of Orthopaedic Science*, *10*(3), 302–307.

Makita, N., Suzuki, M., Asami, S., Takahata, R., Kohzaki, D., Kobayashi, S., et al. (2008). Two of four alternatively spliced isoforms of RUNX2 control osteocalcin gene expression in human osteoblast cells. *Gene*, *413*(1–2), 8–17.

Massia, S. P., & Hubbell, J. A. (1990). Covalently attached GRGD on polymer surfaces promotes biospecific adhesion of mammalian cells. *Annals of the New York Academy of Sciences*, *589*, 261–270.

Mathews, S., Gupta, P. K., Bhonde, R., & Totey, S. (2011). Chitosan enhances mineralization during osteoblast differentiation of human bone marrow-derived mesenchymal stem cells, by upregulating the associated genes. *Cell Proliferation*, *44*(6), 537–549.

Muzzarelli, R. A. A. (2009a). Chitins and chitosans for the repair of wounded skin, nerve cartilage and bone. *Carbohydrate Polymers*, *76*, 167–182.

Muzzarelli, R. A. A. (2009b). Genipin-crosslinked chitosan hydrogels as biomedical and pharmaceutical aids. *Carbohydrate Polymers*, *77*, 1–9.

Muzzarelli, R. A. A. (2011). Chitosan composites with inorganics,morphogenetic proteins and stem cells, for bone regeneration. *Carbohydrate Polymers*, *83*(4), 1433–1445.

Otto, F., Thornell, A. P., Crompton, T., Denzel, A., Gilmour, K. C., Rosewell, I. R., et al. (1997). Cbfa1, a candidate gene for cleidocranial dysplasia syndrome, is essential for osteoblast differentiation and bone development. *Cell*, *89*(5), 765–771.

Peniche, C., Fernadez, M., Rodriguez, G., Parra, J., Jimenez, J., Lopez Bravo, A., et al. (2007). Cell supports of chitosan/hyaluronic acid and chondroitin sulphate systems. Morphology and biological behaviour. *Journal of Materials Science – Materials in Medicine*, *18*(9), 1719–1726.

Phillips, A. M. (2005). Overview of the fracture heating cascade. *Injury – International Journal of the Care of the Injured*, *36*, 5–7.

Pittenger, M. F., Mackay, A. M., Beck, S. C., Jaiswal, R. K., Douglas, R., Mosca, J. D., et al. (1999). Multilineage potential of adult human mesenchymal stem cells. *Science*, *284*(5411), 143–147.

Schroeder, T. M., Jensen, E. D., & Westendorf, J. J. (2005). Runx2: A master organizer of gene transcription in developing and maturing osteoblasts. *Birth Defects Research. Part C: Embryo Today: Reviews*, *75*(3), 213–225.

Shin, H., Temenoff, J. S., Bowden, G. C., Zygourakis, K., Farach-Carson, M. C., Yaszemski, M. J., et al. (2005). Osteogenic differentiation of rat bone marrow stromal cells cultured on Arg-Gly-Asp modified hydrogels without dexamethasone and beta-glycerol phosphate. *Biomaterials*, *26*(17), 3645–3654.

Tsai, W. B., Chen, C. H., Chen, J. F., & Chang, K. Y. (2006). The effects of types of degradable polymers on porcine chondrocyte adhesion, proliferation and gene expression. *Journal of Materials Science: Materials in Medicine*, *17*(4), 337–343.

Tsai, W. B., Chen, R. P., Wei, K. L., Chen, Y. R., Liao, T. Y., Liu, H. L., et al. (2009). Polyelectrolyte multilayer films functionalized with peptides for promoting osteoblast functions. *Acta Biomaterialia*, *5*(9), 3467–3477.

Tsai, W. B., Chen, R. P., Wei, K. L., Tan, S. F., & Lai, J. Y. (2010). Modulation of RGD-functionalized polyelectrolyte multilayer membranes for promoting osteoblast function. *Journal of Biomaterials Science: Polymer Edition*, *21*(3), 377–394.

Tsai, W. B., Chen, Y. R., Liu, H. L., & Lai, J. Y. (2011). Fabrication of UV-crosslinked chitosan scaffolds with conjugation of RGD peptides for bone tissue engineering. *Carbohydrate Polymers*, *85*(1), 129–137.

VandeVord, P. J., Matthew, H. W., DeSilva, S. P., Mayton, L., Wu, B., & Wooley, P. H. (2002). Evaluation of the biocompatibility of a chitosan scaffold in mice. *Journal of Biomedical Materials Research*, *59*(3), 585–590.

Venkatesan, J., & Kim, S. K. (2010). Chitosan composites for bone tissue engineering – An overview. *Marine Drugs*, *8*(8), 2252–2266.

Wang, P. Y., Chow, H. H., Lai, J. Y., Liu, H. L., & Tsai, W. B. (2009). Dynamic compression modulates chondrocyte proliferation and matrix biosynthesis in chitosan/gelatin scaffolds. *Journal of Biomedical Materials Research. Part B: Applied Biomaterials*, *91*(1), 143–152.

Wang, P. Y., Chow, H. H., Tsai, W. B., & Fang, H. W. (2009). Modulation of gene expression of rabbit chondrocytes by dynamic compression in polyurethane scaffolds with collagen gel encapsulation. *Journal of Biomaterials Applications*, *23*(4), 347–366.

Wang, P. Y., Tsai, W. B., & Voelcker, N. H. (2012). Screening of rat mesenchymal stem cell behaviour on polydimethylsiloxane stiffness gradients. *Acta Biomaterialia*, *8*(2), 519–530.

Yang, F., Williams, C. G., Wang, D. A., Lee, H., Manson, P. N., & Elisseeff, J. (2005). The effect of incorporating RGD adhesive peptide in polyethylene glycol diacrylate hydrogel on osteogenesis of bone marrow stromal cells. *Biomaterials*, *26*(30), 5991–5998.

Yang, X., Chen, X., & Wang, H. (2009). Acceleration of osteogenic differentiation of preosteoblastic cells by chitosan containing nanofibrous scaffolds. *Biomacromolecules*, *10*(10), 2772–2778.